Bulletin of the Seismological Society of America, Vol. 99, No. 1, pp. 268–276, February 2009, doi: 10.1785/0120080122

# Calibration of an $M_L$ Scale in the Alborz Region, Northern Iran

by Roohollah Askari, Abdolreza Ghods, and Farhad Sobouti

Abstract We have calculated empirical attenuation curves for the local magnitude scale ($M_L$) in the Alborz region of northern Iran. The maximum trace amplitudes derived from synthetic Wood–Anderson seismograms of 1290 records of 59 events in the distance range of 8.5–550 km recorded by the short-period Iranian Seismic Telemetry Network (ISTN) were inverted for the attenuation curve, magnitudes, and station corrections. The earthquakes ranged from $M_L$3.25 to 5.65 and were recorded at 26 stations in the region. We used both nonparametric and parametric least-squares methods for inversion. The resulting parametric equation is $\log A_0 = -1.1725 \log(R) - 0.0021R - 0.4450$. The two methods yielded very similar results and are very close to Richter's original attenuation curve for southern California. The station corrections vary between $-0.42$ and $+0.47$ suggesting that local site effects may have a strong influence on the amplitudes.

## Introduction

The Alborz range of northern Iran (Fig. 1) is a zone of intense active deformation and seismicity. It is part of the Arabia–Eurasia collision zone where deformation is characterized by partitioning of strain into range-parallel left-lateral strike-slip faulting and thrust faults (Jackson *et al.*, 2002; Allen *et al.*, 2003). Seismicity in the Alborz, like many other regions of Iran, is mostly limited to the upper 20 km of the crust. The Alborz is the most heavily populated region of Iran, including Tehran with a population of over 10 million. The region is affected by numerous active faults, some of them with great seismic potential and documented historical seismicity (Ambraseys and Melville, 1982; Berberian and Yeats, 1999). As such, the Alborz region is a prime candidate for seismic hazard evaluation studies.

The $M_L$ is commonly used in engineering because it is determined within the frequency range (1–5 Hz) of interest to most such applications. For any comprehensive seismic hazard analysis one needs a calibrated magnitude relationship as well as an earthquake catalog for the study region. It is a well-known fact that regional geology has great influence on magnitude relations. Therefore, for each seismic region a specific magnitude relation has to be developed. Currently, seismicity in the Alborz is being monitored by two permanent networks: the short-period Iranian Seismic Telemetry Network (ISTN) and the broadband Iranian National Seismic Network (INSN). Neither network uses magnitude relationships calibrated specifically for Iran. The ISTN uses the Nuttli (1973) magnitude relationship developed for eastern North America. The INSN uses the Hutton and Boore (1987) $M_L$ scale calibrated for southern California. Developing a $M_L$ scale specific to the Alborz region can, therefore, provide a more solid foundation for future seismic hazard studies in Tehran and other centers of population in northern Iran.

Shoja-Taheri *et al.* (2007) derived an $M_L$ scale for the Iranian plateau using the strong-motion data recorded by the National Strong-Motion Network of Iran (NSMNI). They divided their study region into three segments, and the Alborz region fell in their northern segment. Their $M_L$ relationship is limited to distances smaller than 200 km and is based on rather large events ($M > 4.5$). Therefore, their ray coverage was nonuniform and in some places not dense enough. The stations of NSMNI are mostly located on soft platforms or inside buildings. Therefore, their amplitudes may be significantly amplified by soft layers beneath them or by soil–structure interactions. For this reason, magnitude scales calibrated using strong-motion networks might differ to some extent from that derived from seismic networks that are normally stationed on hard bedrock with much smaller site amplification.

The availability of a relatively large volume of short-period data from northern Iran motivated us to calibrate a new $M_L$ scale for the Alborz region. In the following, we first introduce the ISTN and then explain the procedure for calculating the $M_L$ scale. We also report magnitude corrections ISTN stations in the study area.

## Data

The analysis presented in this article is based on the data collected by the ISTN (see the Data and Resources section). Founded in 1995 by the Institute of Geophysics of the University of Tehran, the ISTN is the first modern seismic network of Iran. The network is equipped with three-component short-period SS-1 seismometers (made by Kinemetrics) with

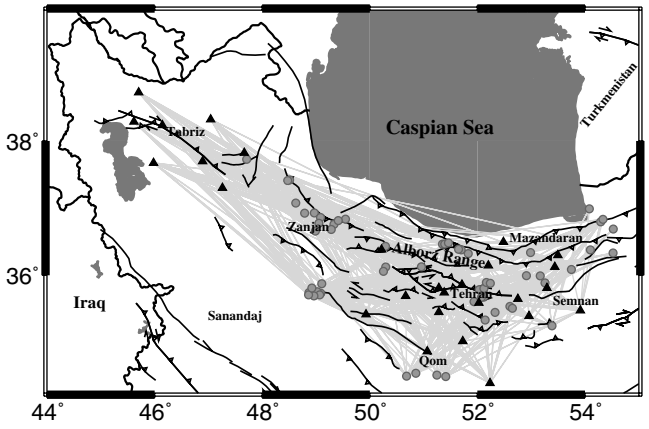


**Figure 1.** Map of the study area. The solid black lines show the traces of the active faults in the region; triangles are the stations of ISTN; circles are the epicenters of the events used in this study; and gray lines are the surface trace of the event-station paths.

eigenfrequency of 1 Hz and 24 or 16 bit digitizers with a sampling rate of 50 sample/sec. The network is made up of several provincial subnetworks. Ghods and Sobouti (2005) give a detailed description of the hardware and the network setup of ISTN. Our study area encompasses the Alborz range and the plain regions to the south of it that are part of the northern margins of the central Iranian block. Three of the subnetworks, Mazandaran, Semnan, and Tehran, cover this area (see Fig. 1). In addition, we used the data of the Tabriz subnetwork to the northwest of the region. The Tabriz network is one of the two oldest subnetworks (along with the Tehran network) and has accumulated a fairly large amount of data in the last 10 yr. The four subnetworks have a total of 26 stations. The average interstation distance inside the Alborz region (that is, excluding the Tabriz stations) is about 50 km.

The data used in this study are 1290 records of 59 earthquakes that occurred in the period 1996–2007 (Fig. 1 and Table 1). In order to increase the location accuracy of the events, we first combined all the data from all the subnetworks and relocated the events. For those events that lie closer to the corners of the study area, we used phase readings from neighboring subnetworks to the south. The magnitudes of the events range from 3.25 to 5.73 as calculated from Hutton and Boore's (1987) $M_L$ relationship (see Table 1). We chose events of $M < 6$ to avoid the problem of saturation of the $M_L$ scale for large magnitudes (Bormann *et al.*, 2002). Figure 2 shows the distribution of magnitudes versus hypocentral distances. To insure good signal-to-noise ratios for amplitude measurements, we did not use events of $M < 3.25$. The events were selected to provide relatively homogenous ray coverage inside the study area. The epicentral location error for the events is less than 5 km. The hypocentral depths have poorer accuracy. Most are around 15 km, which is in agreement with the pattern of seismicity in the region (Bondar *et al.*, 2004). The Alborz is a zone of compressional deformation, and seismicity is mostly limited to the upper 20 km of the crust.

## Determination of the Attenuation Curve

Richter's (1935, 1958) $M_L$ formula first developed for southern California is defined as

$$M_L = \log A(R) - \log A_0(R), \tag{1}$$

where $A(R)$ is the maximum amplitude (in millimeters) at a hypocentral distance of $R$ (in kilometers), and $\log A_0(R)$ is the empirically derived attenuation curve. The attenuation curve depends on anelasticity, scattering, and geometrical spreading along the event-station path. One important task is to obtain a mathematical representation of $\log A_0(R)$. This can be accomplished by fitting a parametric or nonparametric attenuation function to the observed amplitudes. The parametric method assumes a specific functional dependence of $\log A_0(R)$ on $R$ and tries to fit that function to the data. The nonparametric method assumes no specific form of $\log A_0(R)$, and the shape of the attenuation curve is determined by the data. Bakun and Joyner (1984) and Hutton and Boore (1987) adopted a parametric least-squares fitting technique for central and southern California, respectively, and since then many others have followed their methodology. The parametric expression as given by Bakun and Joyner (1984) has the following form:

$$\log A_{ij} = -n \log R_{ij} - \sum_{l=1}^{\text{stations}} S_l \delta_{lj} + \sum_{k=1}^{\text{events}} C_k \delta_{ik}, \tag{2}$$

where $A_{ij}$ is the amplitude of event $i$ recorded at station $j$, $R_{ij}$ is the event-station hypocentral distance, $n$ is the geometrical spreading coefficient ($A \sim 1/R^n$), $K$ is the attenuation coefficient ($A \sim e^{-\ln 10 KR}$), $S_l$ are the station correction terms constrained to sum to zero, $\delta$ is the Kronecker delta function, and $C_k$ are related to earthquake magnitude and are constrained by Richter's criterion that a zero magnitude earthquake should have an amplitude of 0.001 mm at a 100 km distance from the epicenter.

Savage and Anderson (1995) introduced a nonparametric least-squares inversion method, which has been used by others (e.g., Kim, 1998). In this method, the amplitudes recorded at arbitrary distances are linearly interpolated to yield values for the attenuation curve at some fixed distances. The number of the fixed points for which $\log A_0$ is calculated depends on the density of amplitude readings over the distance range considered. Unlike the parametric method, the nonparametric method does not impose any *a priori* assumption of the shape of the attenuation curve on the data and has the potential to detect hinges in the attenuation curve that are caused by structural boundaries such as the Moho. Savage and Anderson (1995) rewrote equation (1) in the following matrix form:

Table 1

The Catalog of the Earthquakes Used in This Study

| Date (yyyy/mm/dd) | Time (UTC) | Latitude | Longitude | Depth (km) | $M_L$ | $M_L^*$ |
|---|---|---|---|---|---|---|
| 1996/06/25 | 14:11 | 37.427 | 48.509 | 15.0 | 3.74 | 3.81 |
| 1996/11/18 | 14:02 | 36.123 | 50.297 | 22.0 | 3.61 | 3.63 |
| 1997/03/18 | 05:35 | 35.782 | 52.035 | 10.0 | 3.69 | 3.71 |
| 1997/04/25 | 18:11 | 35.435 | 52.330 | 15.0 | 3.78 | 3.79 |
| 1997/10/22 | 19:29 | 36.433 | 50.292 | 15.0 | 3.63 | 3.69 |
| 1998/02/24 | 12:27 | 36.842 | 49.550 | 14.7 | 3.60 | 3.66 |
| 1998/04/20 | 02:49 | 36.765 | 49.335 | 16.8 | 3.83 | 3.89 |
| 1998/10/09 | 20:13 | 36.933 | 48.791 | 16.2 | 3.55 | 3.62 |
| 1998/12/03 | 21:07 | 36.128 | 50.961 | 10.0 | 3.93 | 4.00 |
| 1999/01/27 | 09:55 | 36.935 | 48.969 | 17.4 | 3.83 | 3.89 |
| 1999/07/12 | 03:43 | 35.601 | 51.938 | 12.9 | 3.49 | 3.48 |
| 1999/07/14 | 05:12 | 37.732 | 47.712 | 11.0 | 3.81 | 3.84 |
| 1999/07/21 | 03:58 | 36.868 | 49.085 | 15.0 | 3.73 | 3.79 |
| 1999/09/05 | 03:57 | 35.800 | 52.121 | 10.0 | 3.79 | 3.80 |
| 2000/02/28 | 18:43 | 37.081 | 48.624 | 16.7 | 3.60 | 3.67 |
| 2000/08/16 | 12:52 | 36.802 | 54.291 | 15.0 | 5.14 | 5.18 |
| 2000/09/05 | 15:01 | 37.417 | 48.475 | 15.0 | 3.84 | 3.92 |
| 2001/02/16 | 01:43 | 35.320 | 52.144 | 17.2 | 3.73 | 3.72 |
| 2001/02/16 | 10:45 | 35.891 | 52.167 | 15.0 | 3.34 | 3.33 |
| 2001/03/04 | 11:45 | 35.233 | 53.388 | 15.0 | 4.38 | 4.39 |
| 2001/06/24 | 07:05 | 35.879 | 52.240 | 17.4 | 3.64 | 3.64 |
| 2001/07/24 | 20:45 | 34.460 | 50.682 | 15.0 | 3.74 | 3.79 |
| 2001/09/12 | 04:38 | 34.454 | 51.414 | 15.0 | 3.71 | 3.75 |
| 2001/11/17 | 21:19 | 35.885 | 53.257 | 15.0 | 3.47 | 3.48 |
| 2002/02/12 | 05:27 | 35.668 | 52.117 | 17.1 | 3.68 | 3.68 |
| 2002/03/09 | 18:28 | 35.993 | 52.911 | 15.0 | 3.74 | 3.75 |
| 2002/05/21 | 10:48 | 36.381 | 51.701 | 17.0 | 3.96 | 3.98 |
| 2002/06/25 | 06:51 | 35.729 | 49.087 | 15.0 | 3.81 | 3.88 |
| 2002/06/26 | 18:51 | 35.736 | 48.869 | 15.0 | 3.67 | 3.73 |
| 2002/07/ 03 | 19:24 | 35.714 | 48.934 | 16.2 | 4.00 | 4.10 |
| 2002/07/07 | 18:50 | 35.991 | 53.168 | 16.3 | 3.79 | 3.81 |
| 2002/07/20 | 15:22 | 35.749 | 49.024 | 15.0 | 3.76 | 3.84 |
| 2002/07/23 | 17:59 | 35.702 | 49.071 | 15.0 | 3.74 | 3.81 |
| 2002/08/04 | 09:40 | 36.327 | 51.830 | 26.2 | 3.69 | 3.70 |
| 2002/08/23 | 00:49 | 35.871 | 49.108 | 15.0 | 3.90 | 3.97 |
| 2002/09/17 | 02:02 | 34.478 | 51.248 | 15.0 | 3.79 | 3.81 |
| 2002/12/15 | 16:34 | 35.686 | 48.962 | 15.8 | 3.62 | 3.69 |
| 2003/02/24 | 15:48 | 36.086 | 53.747 | 15.0 | 3.75 | 3.76 |
| 2003/03/14 | 05:04 | 35.664 | 52.076 | 15.0 | 3.56 | 3.56 |
| 2003/06/22 | 03:39 | 35.526 | 52.605 | 16.4 | 4.23 | 4.26 |
| 2003/06/22 | 22:03 | 35.498 | 52.650 | 15.0 | 3.59 | 3.61 |
| 2003/09/30 | 15:32 | 36.340 | 52.989 | 15.0 | 3.88 | 3.92 |
| 2003/10/13 | 22:42 | 36.822 | 49.416 | 15.0 | 3.61 | 3.68 |
| 2004/03/06 | 20:00 | 36.780 | 49.053 | 15.0 | 3.54 | 3.61 |
| 2004/05/28 | 17:34 | 36.469 | 51.35 | 16.0 | 3.83 | 3.89 |
| 2004/05/29 | 04:12 | 36.392 | 51.65 | 31.3 | 3.65 | 3.71 |
| 2004/05/31 | 22:05 | 36.467 | 51.395 | 24.1 | 3.55 | 3.57 |
| 2004/06/07 | 04:01 | 36.488 | 51.461 | 16.4 | 3.98 | 4.03 |
| 2004/07/23 | 12:21 | 36.663 | 48.987 | 15.0 | 3.93 | 4.00 |
| 2005/04/14 | 08:44 | 36.687 | 49.283 | 14.7 | 3.73 | 3.79 |
| 2006/01/05 | 13:01 | 35.703 | 48.864 | 15.0 | 3.66 | 3.74 |
| 2006/02/17 | 17:46 | 36.335 | 54.524 | 15.0 | 3.25 | 3.33 |
| 2006/02/22 | 23:19 | 36.057 | 50.253 | 15.0 | 4.02 | 4.07 |
| 2006/06/28 | 14:11 | 35.807 | 48.922 | 15.0 | 3.83 | 3.89 |
| 2006/11/02 | 00:58 | 36.84 | 54.333 | 16.1 | 3.49 | 3.56 |
| 2006/11/20 | 08:27 | 36.382 | 54.1 | 15.0 | 3.64 | 3.65 |
| 2007/02/09 | 00:14 | 36.997 | 54.082 | 15.0 | 4.06 | 4.09 |
| 2007/06/18 | 14:29 | 34.506 | 50.855 | 24.4 | 5.73 | 5.80 |
| 2007/09/10 | 04:44 | 36.695 | 54.527 | 15.0 | 3.55 | 3.59 |

The sixth column lists the Hutton and Boore magnitudes. The last column shows magnitudes calculated from our nonparametric method.

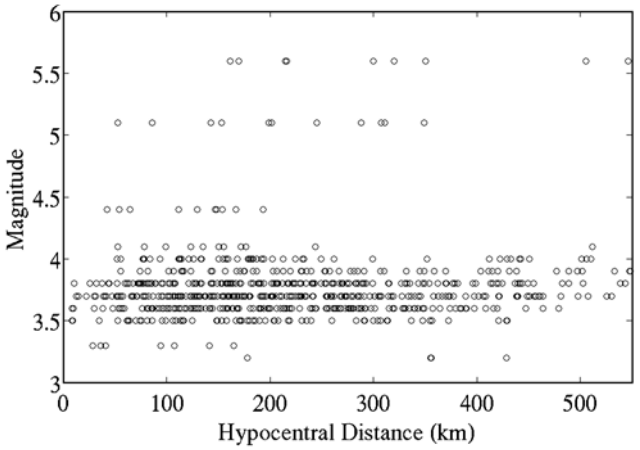


**Figure 2.** Magnitude versus distance for the selected events in this study.

$$a_i = \log_{10} A_0(R_i) + b_j M_j - c_k S_k = \log_{10} A_{jk}(R). \quad (3)$$

Here, $R$ is event-station distance, the indices $j$ and $k$, respectively, refer to events and stations, $M_j$ is the magnitude of event $j$, $S_k$ is the correction term for station $k$, $A_{jk}(R)$ is the amplitude reading for event $j$ at station $k$, and $R_i$ are the fixed distances with spacing $\Delta R = R_{i+1} - R_i$ such that $R_i < R < R_{i+1}$. Coefficients $a_i$, $b_j$, and $c_k$ are weighting factors; $a_i = (R_{i+1} - R)/(R_{i+l} - R_i)$, $a_{i+1} = 1 - a_i$, and all other $a = 0$ for event $j$, $b_j = 1$, and all other $b = 0$ for station $k$, $c_k = 1$, and all other $c = 0$. This method uses linear interpolation of the recorded amplitudes at arbitrary distances to determine the attenuation curve at fixed points. Equation (3) is solved for magnitude, attenuation curve, and station corrections.

In this work we used both the nonparametric method of Savage and Anderson (1995) and the parametric method of Bakun and Joyner (1984) to determine the empirical attenuation curve in the Alborz region. We calculated synthetic W-A seismograms by removing the instrument response of each record and convolving the resulting signal with the response of the standard W-A torsion seismograph. We assumed a static magnification of 2080 for the W-A instrument (as shown by Uhrhammer and Collins [1990], the W-A instrument has a magnification of 2080 and not 2800 as often assumed). The maximum zero-to-peak amplitude was then measured on both horizontal synthetic seismograms. Each component was used separately. This is the procedure used by many others (e.g., Bakun *et al.*, 1978; Kanamori and Jennings, 1978; Uhrhammer and Collins, 1990; Kanamori *et al.*, 1993; Savage and Anderson, 1995). We first discuss the results obtained by the nonparametric method in detail and then compare them with that of the parametric method.

## Results of the Nonparametric Method

As can be seen from Figure 2, the number of amplitude readings decrease as the distance grows. We used a smaller spacing of $\Delta R = 40$ km for distances shorter than 480 km and a larger spacing of 70 km for distances between 480 and 550 km. Savage and Anderson (1995) show that calculating the station corrections directly from the inversion or later by averaging the residuals, give very similar results. For this reason and to avoid numerical instabilities, we chose to calculate the station corrections by averaging after the $\log A_0$ and the magnitudes were obtained. Therefore, we set $c$ in equation (3) to zero. In order to make the inversion process stable, we solved equation (3) using an iterative method. We chose our initial solution vector to be one obtained from Hutton and Boore's (1987) relationship. Many workers (e.g., Baumbach *et al.*, 2003) use a direct method to solve equation (3) but constrain the solution to have a small second derivative of $\log A_0$.

Figure 3 shows the attenuation curve derived from the nonparametric method at two spacings of $\Delta R = 25$ km and $\Delta R = 40$ km without station correction. On the curves we imposed Richter's constraint that $\log A_0 = -3$ at $R = 100$ km. Both curves show a general decay with distance with no profound deviations from the overall trend. The lack of any obvious and significant detail suggests that the crustal structure and geological variations have minimum effect on the shape of the attenuation curve. This does not mean that there is no amplification due to late arriving phases (Burger *et al.*, 1987). The resolution of the attenuation curve (40 km and less) may not allow us to detect amplification of amplitudes that are normally observed with small spacing intervals. $\Delta R = 40$ km gives a somewhat smoother variation consistent with the conclusion reached by Savage and Anderson (1995) that larger spacings give smoother curves. In our data, average interstation distance is 50 km, and the bulk of the data has event-station distances between

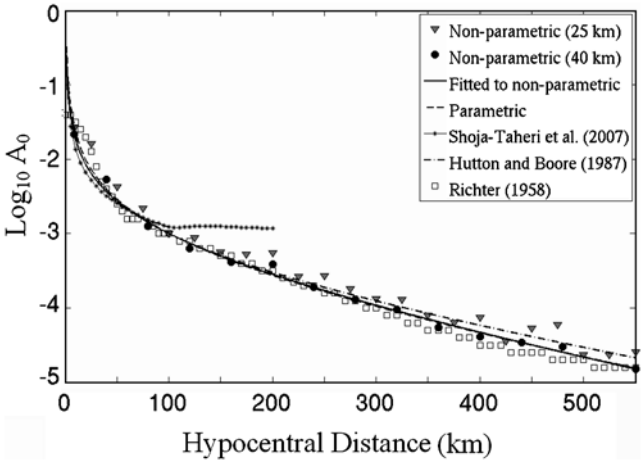


**Figure 3.** Comparison of attenuation curves calculated in this study. Triangles are nonparametric curve with $\Delta R = 40$ km; circles are nonparametric curve with $\Delta R = 25$ km; solid line is curve fitted to nonparametric result with $\Delta R = 40$ km; dashed line is parametric curve; stars are curve obtained by Shoja-Taheri *et al.* (2007); dash-dottted line is Hutton and Boore's (1987) curve for southern California; and squares are Richter's (1958) curve.

50 and 350 km. Therefore, it should not be surprising that a spacing of 40 km gives a smoother curve. We later show that $\Delta R = 40$ km is the optimum model among all models tested. Figure 3 also shows Richter's (1958) original attenuation curve as well as that of Hutton and Boore (1987) for southern California. It can be seen that the difference between our curve and Richter's curve is very small over the entire hypocentral interval and never exceeds 0.25 unit of magnitude. For $R < 50$ km, our curve gives smaller $\log A_0$ values than Richter's curve. Between $R = 40$ and $R =$ 350 km, the two curves are very close to each other, and beyond $R = 350$ km our curve gives slightly larger $\log A_0$ values. Comparing the results with Hutton and Boore's (1987) parametric curve, one would have difficulty choosing between the Richter and Hutton and Boore curves, as both are very close to our curve. For $R < 250$ km, there is very close agreement between our curve and that of Hutton and Boore. At $R > 250$ km, Hutton and Boore's curve gives larger values by up to 0.25 units.

For a given event, the $M_L$ is independently calculated for each recording station. The $M_L$ for the event is then determined as the arithmetic mean of the $M_L$ of all stations. The residual between the mean magnitude of earthquake $i$, $\tilde{M}_i$, and the magnitude calculated for station $j$, $M_{ij}$, is

$$\mathrm{res}(M_L)_{ij} = \tilde{M}_i - M_{ij}. \quad (4)$$

Figure 4 shows the residuals and their mean values for the $\Delta R = 40$ km curve. The mean values were calculated by averaging the residuals in 40 km distance intervals. The residuals and their mean values have a uniform distribution with distance and follow the zero baseline very closely. This confirms that our attenuation curve can successfully model the relationship between attenuation and hypocentral distance in the region. Figure 5a shows residuals versus magnitude. There is no discernible trend in the variations of the residuals with magnitude, and thus, there is no dependency on magnitude. Figure 6 shows the residuals and their mean for the Alborz region as calculated from Hutton and Boore's (1987) formula. From the slope of the best-fitting straight lines, it can be seen that Hutton and Boore's formula gives somewhat larger residues for magnitude estimates.

In the absence of any kinks in the nonparametric curve obtained here, we can closely fit the following curve to the nonparametric result for $\Delta R = 40$ km:

$$\log A_0 = -1.0570 \log(R) - 0.0023R - 0.6556. \quad (5)$$

This curve has the same form as the parametric curve fitting. One reason for such a curve fitting would be to provide a seismic network a formula for magnitude determination. Equation (5) yields $n = 1.0570$ and $K = 0.0023$. In Figure 3, the curve obtained by equation (5) is shown and compared with other results.

To estimate the uncertainties in the calculated $n$ and $K$ parameters, we performed 100 repeated inversions started from bootstrap samples each with 50% of the entire data chosen in random fashion. The bootstrap mean and standard deviation values for $n$ are 1.0661 and $\pm 0.0948$, respectively, and these values for $K$ are 0.0022 and $\pm 0.00002$, respectively. The outcome of the bootstrap tests shows that our inversion procedure is robust with respect to the data. We also tested the sensitivity of the results to the initial assumed solution vector by selecting initial vectors that were signifi-

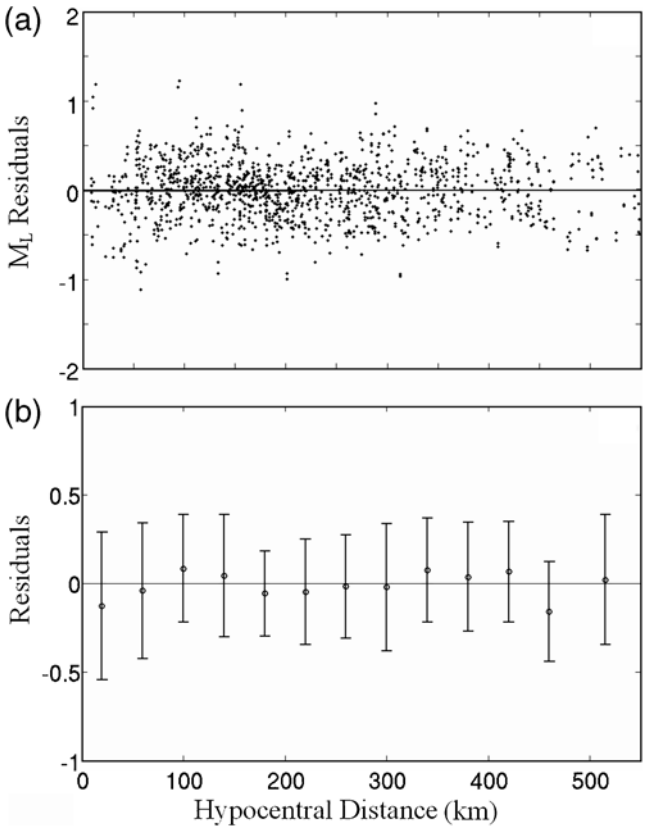


**Figure 4.** (a) Magnitude residuals obtained from the attenuation curve of this study as a function of hypocentral distance. The line is a linear curve fitted to the data. (b) Mean values (circles) and standard deviation (bars) of the magnitude residuals versus distance.

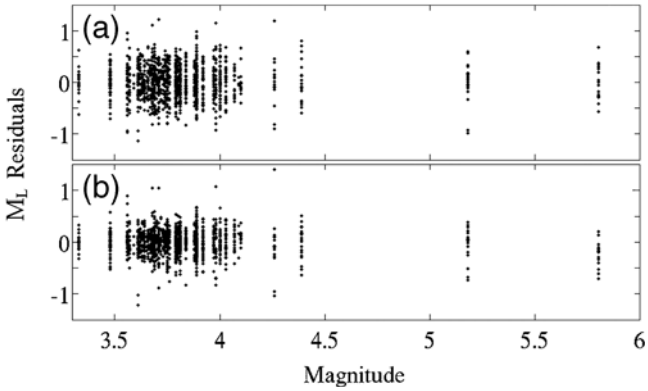


**Figure 5.** Magnitude residuals as a function of magnitudes: (a) results for nonparametric method and (b) results for parametric method.

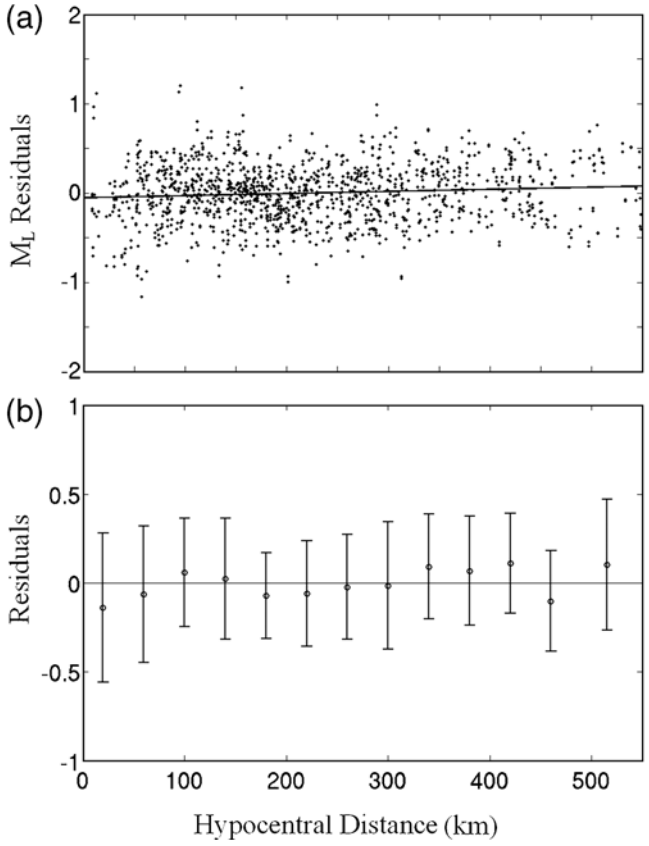


**Figure 6.** (a) Residuals obtained from the attenuation curve introduced by Hutton and Boore (1987) as a function of hypocentral distance. The line is the best-fitting line to the data. (b) Mean values (circles) and standard deviation (bars) of the magnitude residuals with distance.

cantly different (50%–100%) from the Hutton and Boore formula. Perturbation of the initial values only increased the number of iterations; the results were very stable and converged to the same solution. We also checked the sensitivity of the solution to the assumed spacing, $\Delta R$. For each $\Delta R$ we calculated a best-fitting curve like that in equation (5). Table 2 shows the coefficients of equation (5) for different spacing intervals. The mean and standard deviation of magnitude residuals for each model are shown and compared with Hutton and Boore's formula. The standard deviation differs by about 1% among the models with $\Delta R = 40$ having the lowest value.

Table 2

Results of Sensitivity Analysis for Distance Increments Used in the Nonparametric Inversion

| $\Delta R$ (km) | $n$ | $K$ | $c$ | Mean | Standard Deviation |
|---|---|---|---|---|---|
| H-B | 1.110 | 0.00189 | 0.591 | −0.0044 | 0.3232 |
| 25 | 1.075 | 0.00235 | 0.6155 | −0.0077 | 0.3225 |
| 30 | 1.060 | 0.00212 | 0.6496 | −0.0029 | 0.3222 |
| 35 | 1.040 | 0.00237 | 0.6829 | −0.0011 | 0.3230 |
| 40 | 1.057 | 0.00230 | 0.6556 | −0.0023 | 0.3213 |
| 45 | 1.081 | 0.00218 | 0.6204 | −0.0070 | 0.3230 |
| 50 | 1.126 | 0.00193 | 0.555 | −0.0043 | 0.3224 |

The attenuation curve parameters ($n$, $K$, and $c$ in equation 5) and mean and standard deviation of errors in magnitude residuals calculated for our data are shown. The first row shows the results for Hutton and Boore's formula.

We determined a correction term for each recording station by averaging all residuals for that station. Table 3 shows the station corrections. The number of records and standard deviation of magnitude residuals for each station are reported. Station corrections vary between −0.42 to +0.47 among the 26 stations. A range of almost 0.9 unit of magnitude variation suggests that local site effects may have a strong influence on the amplitudes. This is probably true because the stations of the ISTN are founded on very different lithologies. Figure 7 shows the distribution of magnitude residuals after station corrections are enforced. In comparison to Figure 5, we can easily see that station corrections significantly reduce the mean and standard deviation of the residuals in all hypocentral distances. Figure 8 compares the attenuation curve obtained by the nonparametric method before and after station corrections. The difference between the two curves is minimal and at most 0.15 unit of magnitude.

## Results of the Parametric Method

In the second part of our calculations we attempted a parametric fit to the observed amplitudes. We adopted Bakun and Joyner's (1984) methodology but without station correction and obtained the following equation for $\log A_0$ in the Alborz region:

$$\log A_0 = -1.1725 \log(R) - 0.0021R - 0.4450. \qquad (6)$$

The curve was made to observe Richter's constraint that $\log A_0(R = 100) = -3$. The standard deviation of this fit was found to be 0.3215. This number is closest to the standard deviation of the nonparametric model with $\Delta R =$ 40 km (0.3213 in Table 2). In Figure 4 the attenuation curve calculated from equation (6) is shown. There is almost no difference visible between this curve and that fitted to the nonparametric results. We also performed the same bootstrapping tests on the parametric curve. The calculated bootstrap mean and standard deviation for $n$ are 1.1742 and $\pm$0.0559, respectively, and for $K$ are 0.0021 and $\pm$0.0001, respectively. These results show that the estimated attenuation parameters have acceptable accuracy. In Figure 5b, the variation of magnitude residuals with magnitudes for the parametric method are shown. Like in the case of the nonparametric method, the residuals stay fairly uniform over the magnitude range, which suggests that the results are not magnitude dependent.

Shoja-Taheri *et al.* (2007) used strong-motion data to derive an attenuation curve for northern Iran. They first performed a linear regression analysis on their data and obtained a value of $K = -00033$. Because negative values of $K$ are not physically acceptable, they argued that adopting a simple shape for the attenuation curve is insufficient and instead

Table 3
Station Information and Station Correction Values

| Station | Latitude (°N) | Longitude (°E) | Station Correction | Standard Deviation | Number of Records |
|---|---|---|---|---|---|
| AFJ | 35.856 | 51.713 | −0.381 | 0.2162 | 43 |
| ANJ | 35.467 | 53.914 | 0.28 | 0.2268 | 31 |
| AZR | 37.678 | 45.980 | −0.415 | 0.1631 | 36 |
| BST | 37.700 | 46.892 | 0.325 | 0.1818 | 53 |
| DMV | 35.583 | 52.028 | 0.087 | 0.4031 | 81 |
| FIR | 35.641 | 52.754 | 0.258 | 0.2711 | 62 |
| GLO | 36.502 | 53.831 | −0.261 | 0.2576 | 57 |
| GZV | 36.385 | 50.219 | −0.094 | 0.3055 | 55 |
| HRS | 38.318 | 47.042 | 0.099 | 0.111 | 18 |
| HSB | 35.441 | 51.282 | 0.133 | 0.2398 | 69 |
| HSH | 37.307 | 47.263 | 0.008 | 0.283 | 31 |
| KIA | 36.207 | 53.684 | 0.288 | 0.2493 | 48 |
| LAS | 35.382 | 52.959 | 0.193 | 0.2836 | 42 |
| MHD | 35.686 | 50.668 | −0.018 | 0.2283 | 71 |
| MRD | 38.713 | 45.703 | −0.277 | 0.2 | 34 |
| PRN | 36.145 | 52.203 | −0.238 | 0.2463 | 59 |
| QOM | 34.842 | 51.070 | −0.036 | 0.2108 | 70 |
| RAZ | 35.405 | 49.929 | 0.003 | 0.2083 | 69 |
| SFB | 34.354 | 52.236 | 0.174 | 0.1757 | 32 |
| SHB | 38.283 | 45.617 | −0.059 | 0.1835 | 46 |
| SHM | 35.807 | 53.292 | −0.213 | 0.2781 | 41 |
| SHR | 35.806 | 51.283 | −0.248 | 0.1681 | 26 |
| SRB | 37.825 | 47.667 | −0.082 | 0.199 | 38 |
| TBZ | 38.233 | 46.147 | 0.465 | 0.2047 | 40 |
| TEH | 35.737 | 51.382 | −0.02 | 0.2441 | 44 |
| VRN | 34.996 | 51.728 | 0.041 | 0.2243 | 93 |

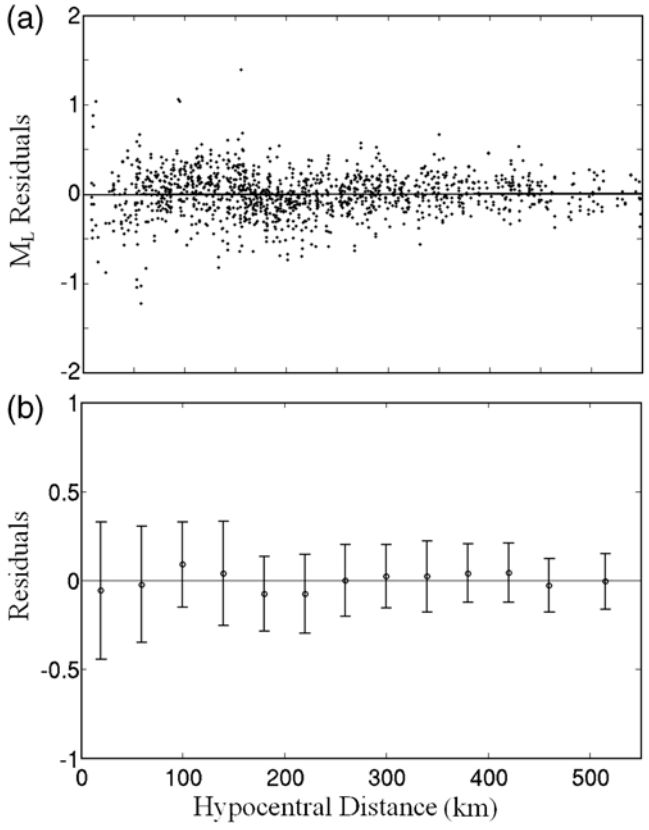


**Figure 7.** (a) Magnitude residuals (dots) obtained from the attenuation curve calculated in this study after enforcing station corrections. (b) Mean values (circles) and standard deviation (bars) of the magnitude residuals with distance.

used a trilinear parametrization of the attenuation curve. Figure 4 compares our curves with that of Shoja-Taheri *et al.* (2007). The two results are significantly different at distances larger than 100 km, which cover the second and third segments of their curve. Furthermore, they obtained a value of $K = 0.00017$ from their trilinear curve, which is an order of magnitude smaller than our estimate of 0.0023. Bakun and Joyner (1984) give the following formula for the $Q/f$ ratio:

$$\frac{Q}{f} = \frac{\pi}{V_S K \ln 10}. \tag{7}$$

Taking an average $S$-wave crustal velocity of $V_S = 3.5$ km/sec, the $K$ value obtained by Shoja-Taheri *et al.* would imply a very large $Q/f$ ratio of 2290 in northern Iran. We believe that this value may be unrealistic for a young collision zone such as the Alborz. Figure 9 shows the magnitudes of the events used in our study as calculated from the two magnitude scales. Clearly, our curve gives higher estimates of magnitude, and the difference can be as large as 0.7 unit of magnitude. We can think of two reasons for the discrepancy between the results of the two studies. First, Shoja-Taheri *et al.*'s region, in addition to the Alborz region, covers the northwestern Iran and parts of northeastern Iran, which are tectonically distinct from the Alborz. Second, and more importantly, our datasets differ in both distance and magnitude ranges. They used strong-motion data in the distance rang of 0–250 km, and the bulk of their data is in the

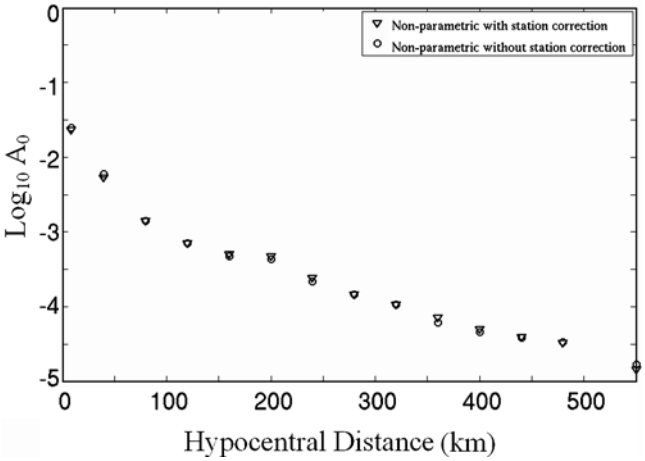


**Figure 8.** Attenuation curve for nonparametric method with $\Delta R = 40$ km, before and after station corrections.

0–75 km range. They used events with $M$ 4.5 and larger and at distances larger than 100 km all of their events are larger than $M$ 5. On the other hand, our data extends up to 550 km, and the bulk of our data is in the 50–350 km interval. Furthermore, small earthquakes are present in all distances (see Fig. 2). As is often the case, strong-motion instruments have smaller number of distant recordings for smaller earthquakes. We believe that Shoja-Taheri *et al.* should add data from higher-gain instruments to their analysis in order to compensate for the underrepresentation of smaller earthquakes at larger distances.

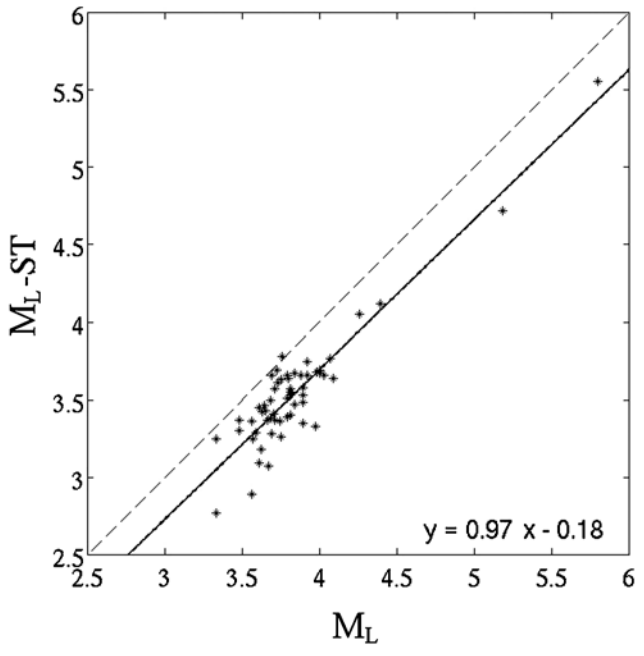


**Figure 9.** $M_L$ of the events used in this study as calculated from the nonparametric method (horizontal axis) versus magnitudes calculated from the formula by Shoja-Taheri *et al.* (2007) (vertical axis). Solid line is straight line fitted to the data.

## Conclusions

An $M_L$ scale was derived for the Alborz region of northern Iran using synthetic W-A seismograms calculated from local networks. We used both parametric and nonparametric curve fittings to the amplitude readings to derive the empirical attenuation curve. The results of the two methods are very similar, and the close agreement between the two curves extends over the entire distance range considered in the study. There was no need to use different curve fitting parameters for different hypocentral intervals in order to make the two curves agree with each other. For this reason we were able to find a single value of geometrical spreading $n$ and a single value of attenuation coefficient $K$ for the entire range considered. This may reflect the fact that the rather large event-station paths used in our study (50–100 km) prevented us from taking into account possible differences in attenuation rate between small and large hypocentral distances.

Our attenuation curves are in close agreement with the Richter (1958) curve. At distances larger than 350 km, Richter's curve gives slightly larger magnitudes (less than 0.25 of a unit). The agreement between our results and that of Hutton and Boore's (1987) for southern California is also very good, although for distances larger than 250 km, the Hutton and Boore formula underestimates magnitude by less than 0.25 unit.

Station corrections calculated in this study range from $-0.42$ to $+0.47$ indicating that local site amplification may have strong influence on magnitude estimates.

## Data and Resources

The data used in this study was obtained from the data bank of the Iranian Seismic Telemetry Network operated by the Institute of Geophysics of the University of Tehran. The bulletin and phase readings can be retrieved from http://irsc.ut.ac.ir (last accessed May 2008). Waveforms can be obtained upon request from the network management.

## Acknowledgments

We would like to express our gratitude towards the Institute of Geophysics of the University of Tehran for allowing us to use ISTN's earthquake data. We thank two anonymous reviewers for constructive criticism and comments.

## References

Allen, M. B., M. R. Ghassemi, M. Shahrabi, and M. Qorashi (2003). Accommodation of late Cenozoic oblique shortening in the Alborz range, northern Iran, *J. Struct. Geol.* **25,** 659–672.

Ambraseys, N. N., and C. P. Melville (1982). *A History of Persian Earthquakes*, Cambridge University Press, London, 219 pp.

Bakun, W. H., S. T. Houck, and W. H. K. Lee (1978). A direct comparison of synthetic and actual Wood–Anderson seismograms, *Bull. Seismol. Soc. Am.* **68,** 1199–1202.

Bakun, W. H., and W. B. Joyner (1984). The $M_L$ scale in central California, *Bull. Seismol. Soc. Am.* **74,** 1827–1843.

Baumbach, M., D. Bindi, H. Grosser, C. Milkereit, S. Parolai, R. Wang, S. Karakisa, S. Zunbul, and J. Zchau (2003). Calibration of an $M_L$ scale

in northwestern Turkey from 1999 Izmit aftershocks, *Bull. Seismol. Soc. Am.* **93,** 2289–2295.

Berberian, M., and R. S. Yeats (1999). Patterns of historical earthquake rupture in the Iranian plateau, *Bull. Seismol. Soc. Am.* **93,** 120–139.

Bondar, I., S. C. Myers, E. R. Engdahl, and E. A. Bergman (2004). Epicentre accuracy based on seismic network criteria, *Geophys. J. Int.* **156,** 483–496.

Bormann, P., M. Baumbach, G. Bock, H. Grosser, G. Choy, and J. L. Boatwright (2002). Seismic Sources and Source Parameters, in *IASPEI New Manual of Seismological Observatory Practice*, P. Bormann (Editor), Vol. **1**, GeoForschungsZentrum, Potsdam, 16–48.

Burger, R., P. Somerville, J. Barker, R. Hermann, and D. Helmberger (1987). The effect of crustal structure on strong ground motion attenuation relations in eastern north America, *Bull. Seismol. Soc. Am.* **77,** 420–439.

Ghods, A., and F. Sobouti (2005). Quality assessment of seismic recording: the Tehran Seismic Telemetry Network, *J. Asian Earth Sci.* **25,** 687–694.

Hutton, L. K., and D. M. Boore (1987). The $M_L$ scale in southern California, *Bull. Seismol. Soc. Am.* **77,** 2074–2094.

Jackson, J. A., K. Priestley, M. B. Allen, and M. Berberian (2002). Active tectonics of the south Caspian basin, *Geol. J. Int.* **148,** 214–245.

Kanamori, H., and P. C. Jennings (1978). Determination of local magnitude, $M_L$, from strong-motion accelerograms, *Bull. Seismol. Soc. Am.* **68,** 471–485.

Kanamori, H., J. Mori, E. Hauksson, T. H. Heaton, L. K. Hutton, and L. M. Jones (1993). Determination of earthquake energy release and $M_L$ using TERRAscope, *Bull. Seismol. Soc. Am.* **83,** 330–346.

Kim, W. Y. (1998). The $M_L$ scale in eastern North America, *Bull. Seismol. Soc. Am.* **88,** 935–951.

Nuttli, O. W. (1973). Seismic wave attenuation relations for eastern North America, *J. Geophys. Res.* **78,** 876–855.

Richter, C. F. (1935). An instrumental earthquake magnitude scale, *Bull. Seismol. Soc. Am.* **25,** 1–32.

Richter, C. F. (1958). *Elementary Seismology*, W. H. Freeman and Co., San Francisco, 758 pp.

Savage, M. K., and J. G. Anderson (1995). A local-magnitude scale for the Western Great Basin-Eastern Sierra Nevada from synthetic Wood Anderson seismograms, *Bull. Seismol. Soc. Am.* **85,** 1236–1243.

Shoja-Taheri, J., S. Naserieh, and H. Ghofrani (2007). $M_L$ and $M_W$ scales in the Iranian Plateau based on the strong-motion records, *Bull. Seismol. Soc. Am.* **97,** 661–669.

Uhrhammer, R. A., and E. R. Collins (1990). Synthesis of Wood-Anderson seismograms from broadband digital records, *Bull Seismol. Soc. Am.* **80,** 702–716.

Department of Physics
Institute for Advanced Studies in Basic Sciences (IASBS), Zanjan
Zanjan, P.O. BOX 45195-1159, Iran
raskari@iasbs.ac.ir
aghods@iasbs.ac.ir
farhads@iasbs.ac.ir

Manuscript received 31 May 2008